

## Sensitivities of a Flash Flood Event over Catalonia: A Numerical Analysis

A. MARTÍN, R. ROMERO, V. HOMAR, A. DE LUQUE, AND S. ALONSO

*Meteorology Group, Department of Physics, Balearic Islands University, Palma de Mallorca, Spain*

T. RIGO AND M. C. LLASAT

*Group of Analysis of Adverse Meteorological Situations (GAMA), Department of Astronomy and Meteorology, University of Barcelona, Barcelona, Spain*

(Manuscript received 9 December 2005, in final form 15 June 2006)

### ABSTRACT

On 9 and 10 June 2000, the northeastern part of the Iberian Peninsula was affected by heavy rains that produced severe floods over densely populated areas. The zones most affected were the provinces of Tarragona and Barcelona, located in the region of Catalonia. Five people were killed, 500 were evacuated, and the property losses were estimated to exceed 65 million euros. The episode was characterized by the entrance of an Atlantic low-level cold front and an upper-level trough that contributed to the generation of a mesoscale cyclone in the Mediterranean Sea east of mainland Spain. The circulation associated with this mesoscale cyclone advected warm and moist air toward Catalonia from the Mediterranean Sea. The convergence zone between the easterly flow and the Atlantic front, as well as the complex orography of the region, are shown to be involved in the triggering and organization of the convective systems. Radar shows the development of two long-lived mesoscale convective systems that merged and remained quasi-stationary nearby the city of Barcelona for nearly 2 h.

The fifth-generation Pennsylvania State University–National Center for Atmospheric Research (PSU–NCAR) Mesoscale Model (MM5) short-range numerical simulations of the episode succeed reasonably well in capturing the accumulated rainfall patterns and important mesoscale aspects of the event. The role of the orography and latent heat release in generating and sustaining the quasi-stationary precipitating systems is assessed through numerical sensitivity analysis. A piecewise potential vorticity inversion technique, assisted by sensitivity fields derived from an adjoint model, provides a test bed to investigate the predictability of the damaging rains given uncertainties in the initial fields. The adjoint results highlight the importance of the details associated with the upper-level precursor trough. Therefore, the effects of small perturbations to the trough intensity and location are also investigated. Interestingly, despite the orography's active role in the generation of the Mediterranean mesoscale cyclone and, hence, on the location of the precipitation maxima, the predictability of the spatial and temporal distribution and amounts of precipitation is shorter than might be expected. This reduced predictability of the rainfall field is attributed to the high sensitivity of the location and depth of the mesoscale cyclone identified in the Mediterranean Sea east of Catalonia to perturbations; that is, to the location and intensity of the precursor upper-level trough, compatible with realistic analysis errors.

### 1. Introduction

Heavy rainfall episodes are a climatic feature of the western Mediterranean (Font 1983; Romero et al. 1999; see Fig. 1 for all locations referred to in the text). Important highly populated areas are affected regularly by

floods that produce human fatalities, substantial property losses, and impacts on the communication systems and landscape. Severe weather events typically occur in the region at the end of the summer (e.g., Homar et al. 2003a) and during autumn (e.g., Doswell et al. 1998; Homar et al. 1999; Ramis et al. 2001), although a few cases are also reported during winter and spring (e.g., January–February, Doswell et al. 1998; May, Riesco et al. 2002; December, Delitala et al. 2002). Highly complex terrain surrounding a quasi-closed sea characterizes the western Mediterranean region. During late

---

*Corresponding author address:* Dr. A. Martín, Meteorology Group, Dept. of Physics, Balearic Islands University, E-07122 Palma de Mallorca, Spain.  
E-mail: alberto.martin@uib.es

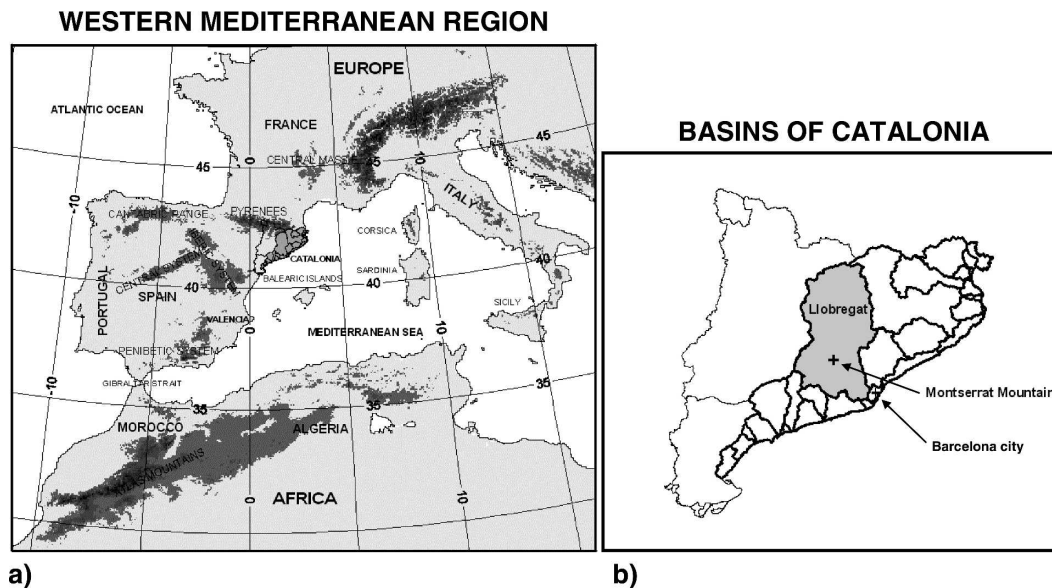


FIG. 1. (a) Western Mediterranean region, showing major topographic features by means of terrain contours (shaded darker gray, intervals of 500 m, starting at 1000 m). The thick continuous line shows Catalonia and inside it, the internal basins of Catalonia (shaded dark gray). (b) Zooming in over Catalonia and its hydrographical basins. The thick continuous line shows the internal basins of Catalonia and the gray basin is the Llobregat River basin, where the maximum rainfall value was recorded.

summer and autumn, the warm sea becomes the primary source of heat and water vapor for heavy precipitating systems. The coastal mountain ranges may not only produce direct action by lifting moist impinging air, but also alter the low-level flow, favoring specific mesoscale processes prone to the development of convection and heavy precipitating systems in the region (e.g., lee cyclones south of the Alps, Buzzi et al. 1998; lee cyclones north of the Atlas, Homar et al. 2002). Typically, the presence of a midlevel cold trough also provides synoptic-scale ascent and destabilization of the low-level airstreams within the mesoscale systems. Many studies document this conceptual model, describing evidences of the interaction of the evaporation from the sea and the uplifting over the adjacent orography in high precipitating episodes: 800 mm in 24 h in Valencia, Spain, on 3 November 1987 (Fernández et al. 1995), more than 400 mm in Catalonia, Spain, on 10 October 1994 (Ramis et al. 1998), and more than 200 mm in Piedmont, Spain, on 5 November 1994 (Doswell et al. 1998).

On 10 June 2000, five people died and more than 500 were evacuated from the monastery of Montserrat. Total material loss, including the destruction of a highway bridge, was estimated to exceed 65 million euros by the media. In fact, this event is cataloged as “catastrophic” by Llasat et al. (2002), fitting their criteria of observed rainfall amounts, total affected area, death toll, and

economic losses (Llasat 2001). The event of 9–10 June 2000 considered in the present study is important because of the extreme rainfall intensities that were observed and the high social impact caused by the resulting flash flood in Catalonia. In fact, this is one of the cases that received the largest attention in the regional media in the twentieth century, with more than 75 references published in 5 local newspapers. This is comparable to only a few historical events, such as the cases of September 1962, September 1981, or October 1982 (Llasat et al. 2003).

Three aspects contributed to this unique flood: the rain rate, the nearly stationary precipitating systems, and the particular terrain configuration of the affected area. Some rain gauges in Catalonia recorded 5-min accumulations reaching 10 mm ( $120 \text{ mm h}^{-1}$ ), with total 6-h amounts of 180 mm. Meteorological radar, situated in Barcelona, Spain, captured the transition of a convective band linked to an Atlantic front to two mesoscale convective systems merging and becoming nearly stationary over Barcelona during the first hours of 10 June. As a consequence of such intense and persistent precipitation over the Llobregat River basin, a prototype western Mediterranean river basin with a complex mosaic of subbasins defined by high and steep slopes, an exceptional flash flood occurred.

Numerical weather forecasts provide important guidance for short-range prediction of the occurrence, lo-

cation, and intensity of heavy rainfall events in the western Mediterranean area (e.g., Romero et al. 2000). Although numerical forecast models can produce highly realistic mesoscale structures, the largely unknown forecast errors reduce the forecaster's confidence in the model fields, especially for convective systems and precipitation (Weiss et al. 2004). The sensitivity of small-scale features in the forecast to errors in the initial and boundary conditions or approximations present in the model, such as the physical parameterizations, determine the degree of predictability of such phenomena in the forecasting system. Basically, all mechanisms involved for the development of heavy precipitating systems in the western Mediterranean region contribute to errors in the numerical forecast. The main purpose of this study is to improve the understanding of existing limitations of numerical forecasts of flash flood situations like the June 2000 episode.

For that purpose it is crucial to identify the factors that play an important role within the synoptic and mesoscale processes associated with the development and organization of the convection. Factors considered in the study include a boundary factor (local and remote orography), a factor associated with the model physics (latent heat flux from the sea), and an internal feature of the upper-level flow dynamics: the precursor short wave trough of the June 2000 episode. Assuming that the mesoscale model is "perfect," we emphasize that the major source of uncertainty in short-range forecasting is associated with a deficient knowledge of the initial conditions ingested in the mesoscale model, because of insufficient observational data (a real problem in the data-void Mediterranean latitudes) and/or an imperfect lower-resolution model forecast to construct the initial conditions. Incorporating the initial conditions uncertainty in the prediction system appears as a basic task for improving the understanding of the predictability of flash flood situations in the western Mediterranean. Homar et al. (2002, 2003b) and Romero (2001) highlight the sensitivity in the location of simulated heavy rains to the positioning of a low-level jet over the Mediterranean, and, hence, indirectly to details in the representation of the precursor upper-level trough in the initial condition fields.

Within this framework, adjoint models can provide valuable information through the computation of quantitative estimations of the sensitivity of forecast aspects to small perturbations in the initial and boundary condition fields. Adjoint models have been used with success to support international adaptive observation campaigns (e.g., Langland et al. 1999a) in mesoscale ensemble generation experiments (Xu et al. 2001) and in

physical sensitivity analysis. Homar and Stensrud (2004) report on the calculation and test of the adjoint-derived sensitivities for a case of intense cyclogenesis over the western Mediterranean. Indeed, comparing the relative impact of lower-boundary factors against initial conditions on the numerical prediction not only allows for better understanding of the physical processes that are involved in the development of heavy rains in the region, but also supports the identification of the most influential sources of uncertainty in the system and provides insight into the role of geographical forcing on the predictability of such damaging episodes.

This paper presents a sensitivity analysis for the fifth-generation Pennsylvania State University–National Center for Atmospheric Research (PSU–NCAR) Mesoscale Model (MM5) numerical simulation for 9 and 10 June 2000, with special attention to the aforementioned dynamical, physical, and lower-boundary factors.

The paper is organized as follows: section 2 describes the observation dataset used, the synoptic situation, and the evolution of convective activity over Catalonia. In section 3, we present the numerical study that provides some details on the main MM5 model characteristics and summarizes the control run results. Section 4 describes the sensitivity experiments and in section 5 we discuss the conclusions of the study.

## 2. Observational analysis

### a. Dataset descriptions

Various observational datasets are used to characterize the heavy precipitating systems observed over Catalonia and to initialize and verify the numerical experiments performed in this study.

- 1) The numerical model is initialized with the global tropospheric analyses from Global Data Assimilation system of the National Centers for the Environmental Prediction (NCEP). They have a  $2.5^\circ \times 2.5^\circ$  latitude–longitude grid spacing and are available every 12 h. These fields are remapped to the model grid by means of an objective analysis that incorporates surface and upper-air observations (Benjamin and Seaman 1985).
- 2) Images from the Barcelona radar of the Spanish Weather Service (Instituto Nacional de Meteorología) are available every 10 min, with 2-km grid spacing and covering an area of  $400 \times 400$  km. Maximum reflectivity (dBZ) images are used to follow the most intense precipitating systems over Catalonia from 2100 UTC 9 June 2000 to 1230 UTC 10

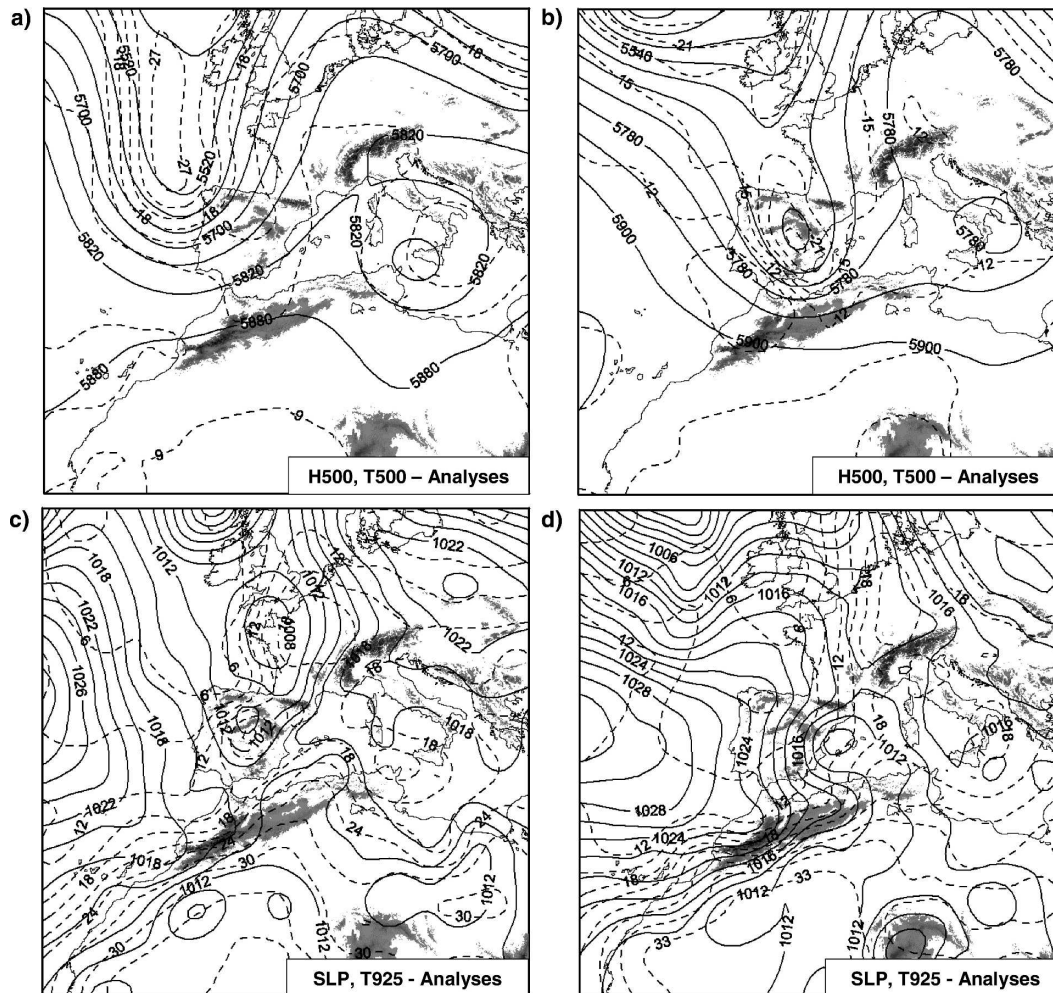


FIG. 2. NCEP analyses maps. (top) Geopotential height at 500 hPa (continuous line, gpm) and temperature at 500 hPa (dashed line, °C) at (a) 0000 UTC 9 Jun 2000 and (b) 0000 UTC 10 Jun 2000. (bottom) Sea level pressure (continuous line, hPa) and temperature at 925 hPa (dashed line, °C) at (c) 0000 UTC 9 Jun 2000 and (d) 0000 UTC 10 Jun 2000. Main orographic systems are highlighted.

June 2000. Attenuation problems occurred from 0300 to 0430 UTC because of the precipitation rates over the radar site, so no acceptable images are available for that period.

- 3) The Automatic System of Hydrological Information of the Catalan Water Agency (ACA) records precipitation of the internal basins of Catalonia at 126 automatic rain gauges every 5 min. These data are used to produce rainfall maps that provide a detailed picture of the evolution and intensity of the precipitating systems.
- 4) An Advanced Very High Resolution Radiometer (AVHRR) image of channels 4 ( $10.30 \mu\text{m} \leq \lambda \leq 11.30 \mu\text{m}$ ) and 5 ( $11.50 \mu\text{m} \leq \lambda \leq 12.50 \mu\text{m}$ ) in the thermal region of the National Oceanic and Atmospheric Administration (NOAA) satellite *NOAA-14*

is used to show the sea surface temperature (SST) over the western Mediterranean on 8 June 2000.

#### b. Synoptic overview

The episode developed under a synoptic pattern characterized by an Atlantic cold upper-level trough progressing from western Europe (Figs. 2a,b) and a low pressure area along the British Islands, western France, and Spain, with an associated cold front extending southward down to northern Africa (Fig. 2c). The front was deformed over the Iberian Peninsula by a warm air mass associated with a secondary low (Fig. 2d). During 9 June, the upper-level short wave trough became negatively tilted and was advecting cold and dry air toward the Iberian Peninsula as the surface cold front advanced east (Figs. 2b,d), producing snowfalls during the

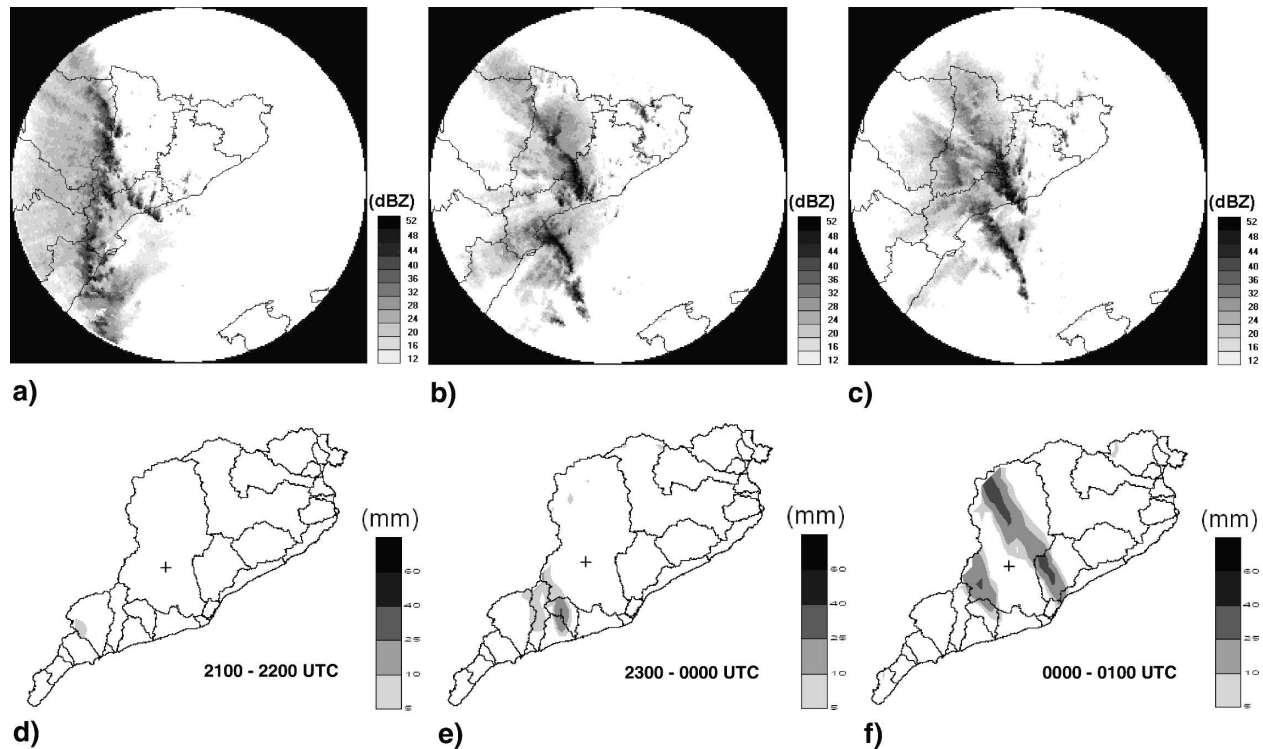


FIG. 3. (top) The Z-max radar maps at (a) 2130 UTC 9 Jun 2000, (b) 2330 UTC 9 Jun 2000, and (c) 0030 UTC 10 Jun 2000. (bottom) Hourly values of accumulated model precipitation in the internal basins of Catalonia (shaded, according to scale, mm) from (d) 2100 to 2200 UTC 9 Jun 2000 (max value is 7 mm), (e) 2300 UTC 9 Jun 2000 to 0000 UTC 10 Jun 2000 (max value is 29 mm), and (f) 0000 to 0100 UTC 10 Jun 2000 (max value is 42 mm). The Montserrat Mountain (cross) is highlighted.

evening over parts of northern Spain. The eastern shift of the secondary low and the influence of cyclonic circulation offshore Algeria favored the entrance of warm advection during the 9 June 2000 and the early hours of 10 June 2000 over Mediterranean Spain (Figs. 2c,d). The cyclonic moist flow established in the western Mediterranean impinged upon the northeastern Spanish littoral, providing a continuous supply of warm and moist air toward the Catalan coast during the second half of 9 June. Thus, the NCEP analysis maps reveal two synoptic and subsynoptic factors favoring intense rains over Catalonia during the first hours of 10 June: (i) a cold midtropospheric trough, accompanied by a surface cold front passage, and (ii) warm and moist southeasterly flow, reinforced by local circulations. The combined action of the warm advection associated with the low-level mesoscale cyclone and the cold advection associated with the midlevel trough led to a convectively unstable environment with high CAPE. The frontal convergence zone was intensified and, together with the impinging maritime flow onto the Catalan coastal mountains, initiated and sustained the precipitation cells. These ingredients will be graphically highlighted in section 3b.

Over the hours following 0000 UTC 10 June 2000, the core of the upper-level Atlantic cold trough overlapped the low-level mesoscale cyclone. As the surface cyclone progressed northeastward into southern France, the winds over Catalonia veered to cold and dry northwesterlies. After 0900 UTC 10 June 2000, heavy rainfall also fell on Mediterranean France (not shown).

### c. Convective activity over Catalonia

The Barcelona radar captured intense organized convective activity over the northeast Iberian Peninsula during the evening of 9 June 2000 and the early hours of 10 June 2000 (see Llasat et al. 2003 for a detailed analysis of the radar imagery for this event). Several thunderstorms are identified at the beginning of the evolution, organizing quickly along the cold frontal zone (not shown).

The first strong radar echoes appeared over Catalonia at about 2130 UTC 9 June 2000 (Fig. 3a). On the 2330 UTC image, two linear mesoscale convective systems (MCSs) could be identified: one north of Valencia and extending eastward over the sea; and the second, over central Catalonia (Fig. 3b). Both systems moved northeastward but the southern one moved faster (Fig. 3c). As a consequence, the systems merged into a

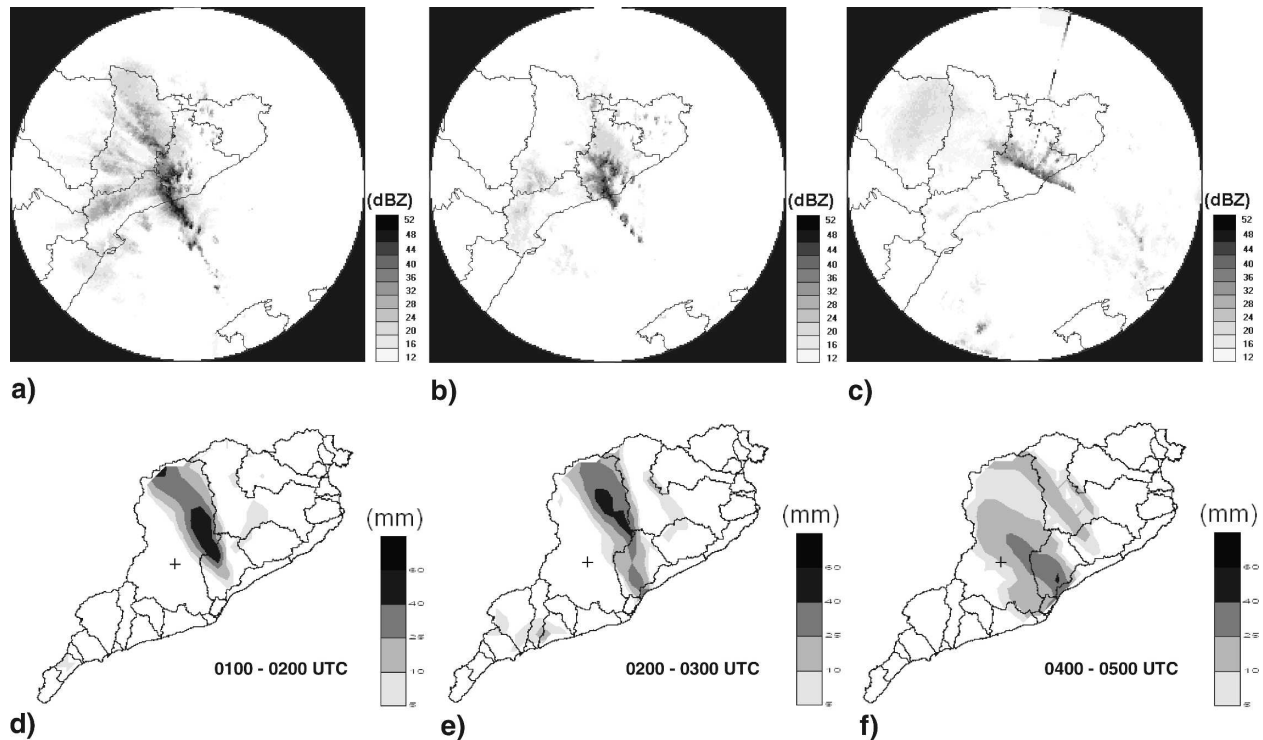


FIG. 4. Same as in Fig. 3, but at (a) 0130, (b) 0230, and (c) 0430 UTC 10 Jun 2000. (bottom) Same as in Fig. 3, but from (d) 0100 to 0200 UTC 10 Jun 2000 (max value is 65 mm), (e) 0200 to 0300 UTC 10 Jun 2000 (max value is 50 mm), and (f) 0400 to 0500 UTC 10 Jun 2000 (max value is 46 mm).

single, larger MCS over southern Catalonia between 0100 and 0130 UTC (Fig. 4a), and continued moving slowly to the northeast. During this period, intense precipitation was recorded in many basins of southern Catalonia such as Francolí, Riera de la Bisbal, Gaia, Foix, or Garraf, where observed rainfall values exceeded 100 mm in less than 2 h. The MCS reached the area of Montserrat at 0230 UTC (Fig. 4b), where the maximum 24-h accumulated rainfall (223 mm) was recorded for this episode (Figs. 5a,b). Then, the system rotated cyclonically around its center for nearly 2 h, with a faster movement over the sea (about  $10 \text{ m s}^{-1}$ ) than over land, resulting in the quasi-stationary character of the precipitation over the Montserrat area. At 0430 UTC, the MCS began to dissipate and the rain rates started decreasing rapidly over Catalonia (Fig. 4c). Later on, a few postfrontal rainfall bands were observed in the region contributing less intense rainfall to the heavy rains already registered (not shown).

### 3. Control experiment

#### a. Numerical setup

Further understanding of this flash flood episode demands an identification and evaluation of mesoscale

processes operating within the synoptic-scale setting presented in the previous section. For this purpose, several simulations were designed using the MM5 (Anthes and Warner 1978; Grell et al. 1994). The MM5 model was developed in the early 1970s and is widely used within the research and operational communities. Its nonhydrostatic dynamics core is derived from the primitive set of equations on a vertical terrain-following sigma coordinate ( $\sigma$ ) and a horizontal projected grid. The equations are integrated over an Arakawa-C staggered grid. It is a versatile modular modeling system with four-dimensional data assimilation and multiple-nest capabilities.

With the aim of accurately simulating fine details of the precipitating systems for this episode, 4 two-way nested domains of 54, 18, 6, and 2 km comprising  $82 \times 82$  grid points were defined, zoomed in over northeastern Spain. The coarse domain is defined in order to describe the evolution of the synoptic pattern, highlight the upper-level precursor trough identified in the episode, and characterize its areas of sensitivity and its primary influence in the configuration of the low-level flow. The second domain is used to capture the most important mesoscale aspects, which led to the damaging heavy rains. The qualitative and quantitative as-

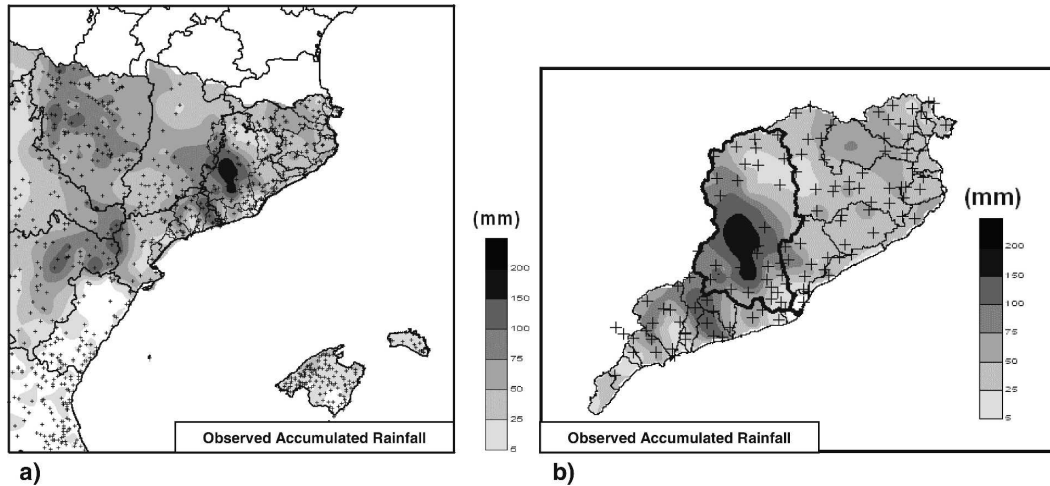


FIG. 5. (a) Observed accumulated rainfall (shaded according to scale, mm) between 0700 UTC 9 Jun 2000 and 0700 UTC 11 Jun 2000. Internal basins of Catalonia (thin continuous line) and the provinces of northeastern Spain and southern France (thick continuous line) are plotted. (b) Observed accumulated rainfall zooming in over the internal basins of Catalonia (shaded according to scale, mm). Maximum value is 223 mm. Rain gauge network (crosses) is highlighted.

pects of the precipitation field are described by the third and fourth domains, which are able to resolve fine aspects of the local topographic forcing. In the vertical, 24  $\sigma$  levels were used, with higher density near the surface to better resolve near-ground processes. The standard version 3 of MM5 distribution incorporates a set of physical parameterizations to represent the sub-grid processes of atmospheric radiation, cloud microphysics, moist convection, turbulent fluxes of energy and momentum, and surface tendencies of temperature and moisture. For the set of simulations presented here, the grid-resolved microphysics processes are represented by the Reisner et al. (1998) scheme, which considers graupel and ice number concentration. The coarse and second domains parameterize convection with the modified Kain–Fritsch scheme (Kain and Fritsch 1993). No cumulus parameterization is used for the third and finest domains. (It could be argued that a convection scheme would still be necessary for the 6-km resolution domain, but our control simulation incorporating the Kain–Fritsch scheme in the third domain produced a worse precipitation field.) Planetary boundary layer (PBL) processes are parameterized with the Medium-Range Forecast PBL Hong–Pan (Hong and Pan 1996) scheme, which is also adequate for high-resolution domains. This is an efficient scheme based on the Troen–Mahrt (Troen and Mahrt 1986) representation of the countergradient term and  $K$  profile in the well-mixed PBL. Atmospheric radiation is parameterized using the Rapid Radiative Transfer Model (longwave scheme; see Mlawer et al. 1997),

which represents the effects of the detailed absorption spectrum taking into account water vapor, carbon dioxide, and ozone. A five-layer diffusive soil model with a fixed substrate below is used. Additionally, moisture availability varies with time, particularly in response to rainfall and evaporation rates. Regarding the initial and boundary condition datasets, the NCEP global analysis data are reanalyzed to the coarse domain every 12 h, incorporating surface and sounding observations with a successive-correction objective analysis technique (Benjamin and Seaman 1985), to recover structures smoothed out in the global datasets. The initial fields for the inner domains are interpolated from the coarser mesh. Lateral boundary conditions on the coarse domain are defined by linear interpolation between the 12-h analyses, and upper boundary conditions are represented by the top vertical motion that is calculated to reduce the reflection of energy and hence prevent spurious noise, especially over prominent orography.

#### b. Results

The heavy rainfall that characterized this case was registered during the first hours of 10 June. Previous sections highlighted the link between the intense convective activity accompanying the cold front passage over Catalonia with the high rainfall rates. To capture the mesoscale details of the evolution of the front as well as the mesoscale cyclone to the east of mainland Spain, a 36-h control simulation, beginning at 0000 UTC 9 June 2000, was run.

The control run reproduces the mesoscale features

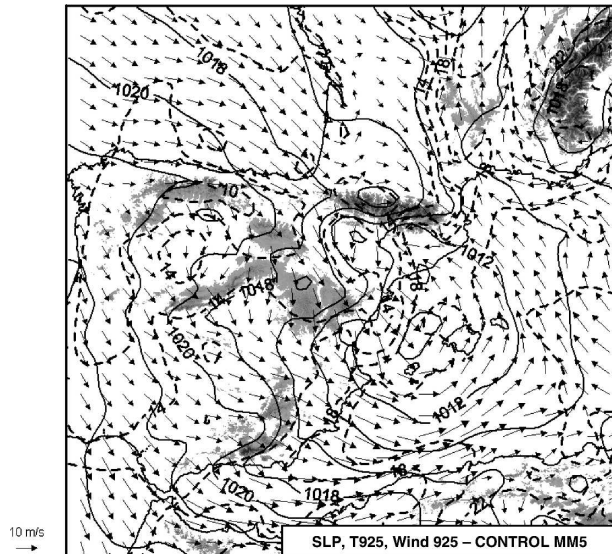


FIG. 6. Control simulation sea level pressure (continuous line, hPa), temperature at 925 hPa (dashed line, °C), and horizontal wind at 925 hPa (vectors) for the second domain at 0000 UTC 10 Jun 2000. Main orographic systems are highlighted.

previously identified as conducive to the damaging heavy rains. In response to the vorticity advection of mid- and upper levels over eastern Spain, as the intense cold trough crosses the Iberian Peninsula from the west, cyclogenesis is simulated leeward of the Iberian system around 1200 UTC 9 June 2000. The low-level wind field reveals various mesoscale circulations converging over central Catalonia (Fig. 6): the cold dry northwesterly frontal winds, the warm moist southeasterly maritime flow supplied by the low-level Mediterranean mesoscale low and the northerly component flow detectable along the eastern flank of the Pyrenees. As a result, strong water vapor flux convergence is detected over the area, a factor of importance to the production of heavy rainfall (Fig. 7). At the same time, superpositioning the cold upper-level trough over the warm and moist low-level southeasterly flow destabilizes the situation, as shown by simulated CAPE values over Catalonia up to  $1000 \text{ J kg}^{-1}$  during the hours preceding convective initiation over the region (Fig. 7). Therefore, the model simulates a scenario with high moisture content throughout a deep column of unstable air (Fig. 7). Candidates for convective initiation mechanisms for this event are the frontal upward motion and the uplift owing to the southeasterly flow impinging toward the local orography (Fig. 8).

The spatial distribution of precipitation over Catalonia is reasonably well reproduced by the control experiment. The simulated 36-h rainfall amounts exceeded 50 mm in most of Catalonia (maximum value is 194 mm,

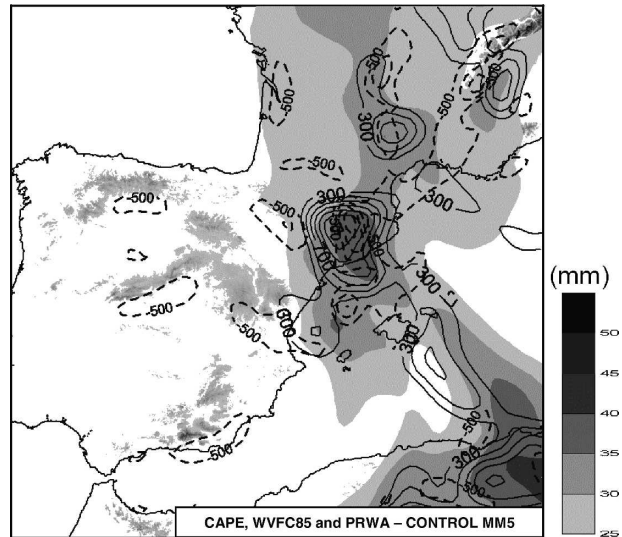


FIG. 7. Control simulation CAPE (continuous line, intervals of  $100 \text{ J Kg}^{-1}$ , starting at  $300 \text{ J Kg}^{-1}$ ), water vapor flux convergence averaged in the 1000–850-hPa layer (dashed line, intervals of  $500 \times 10^{-3} \text{ g m}^{-2} \text{ s}^{-1}$ , starting at  $500 \times 10^{-3} \text{ g m}^{-2} \text{ s}^{-1}$ ) and precipitable water (shaded according to scale, mm) for the second domain at 0000 UTC 10 Jun 2000. Main orographic systems are highlighted.

Fig. 9a), with a band over 200 mm (maximum value is 219 mm, Fig. 9b), which is displaced few kilometers eastward of the observed peak rainfall in Fig. 5b, but is partially located inside the Llobregat basin. A detailed verification of the model precipitation time series with rain gauge and radar measurements shows that the simulated rainfall does not provide an accurate forecast of the details of convection triggering, organization, and evolution (Figs. 3 and 4). In fact, the model does not reproduce the merging of two MCSs and the quasi-stationarity of the convection as observed on the radar, but the high rainfall rates of the episode, which are associated to the frontal upward motion and the orographic uplifting of the southeasterly winds, are well captured by MM5 (Figs. 4d–f). In addition, the main mesoscale flows (see Fig. 2d) that supported the convective developments are well resolved by the control simulation. Therefore, the numerical sensitivity experiments will focus primarily on aspects of the control run that are adequately reproduced.

#### 4. Sensitivity experiments

The complex orography of the western Mediterranean interacts with the synoptic and mesoscale flow and might exert an important effect on the structure and evolution of the weather systems associated with heavy

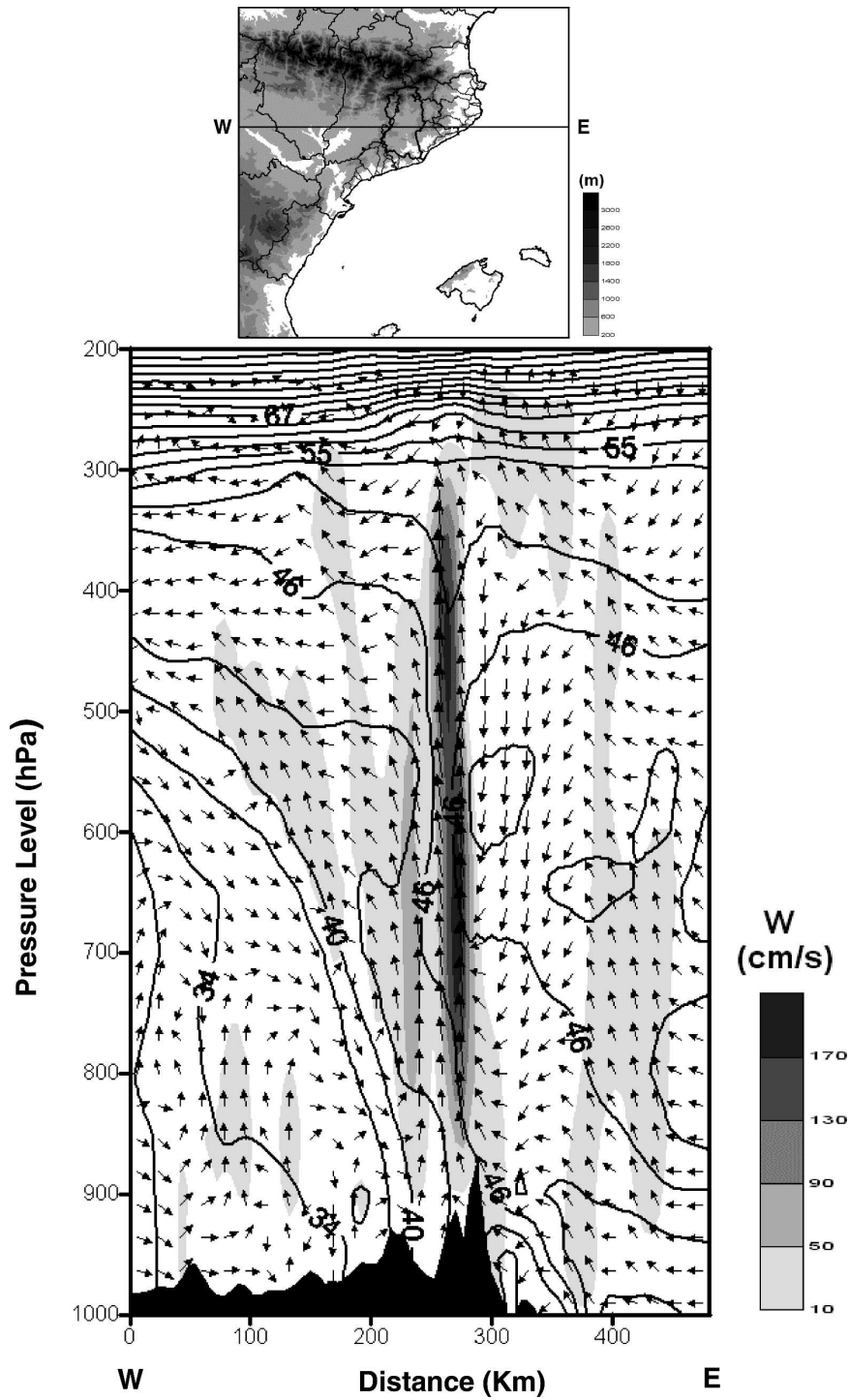


FIG. 8. Control simulation equivalent potential temperature (continuous line, °C), ( $u, w$ ) wind field (vectors) and vertical velocity (shaded according to scale,  $\text{cm s}^{-1}$ ) at 0300 UTC 10 Jun 2000 along a west–east transverse section in the northeastern part of Spain. The highest orography corresponds to the Montserrat area.

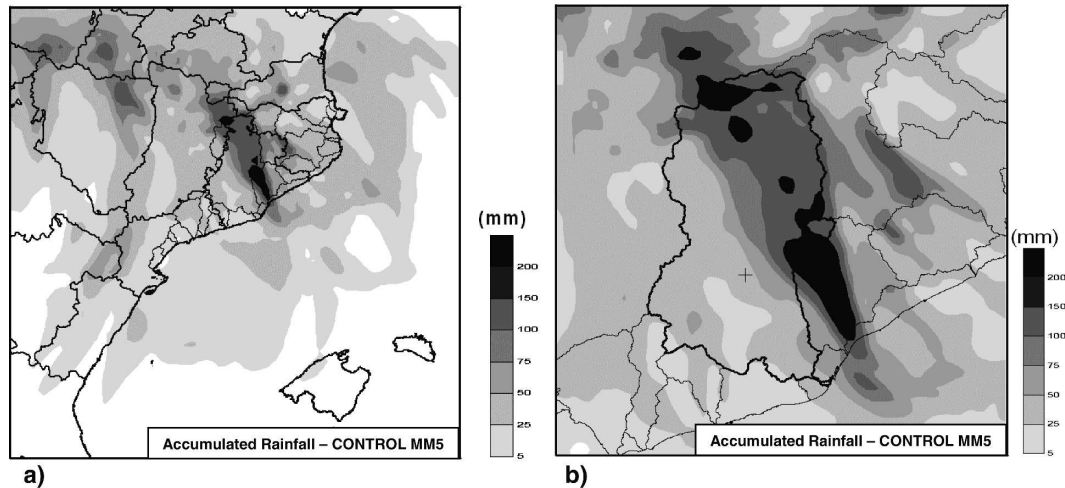


FIG. 9. Control simulation (a) accumulated rainfall (shaded according to scale, mm) for the third domain at the end of the simulation. Maximum value is 194 mm. (b) Accumulated rainfall (shaded according to scale, mm) for the fine domain at the end of the simulation. Maximum value is 219 mm. The Montserrat Mountain (cross) is highlighted.

precipitation. More precisely, a notable coastal range with altitudes of up to 1500 m can be an important factor for the development of convection in Catalonia (Romero et al. 1997).

Several studies (e.g., 28–29 September 1994, Ramis et al. 2001; 12 September 1996, Homar et al. 2003b) show the important role of latent heat flux from the sea in flash flood situations. The warming and moistening of the boundary layer through the latent heat flux from a warm Mediterranean Sea is an efficient mechanism for convective destabilization and the further triggering and maintenance of heavy precipitation. The satellite derived SST on 8 June 2000 reveals an extensive area of

seawater exceeding  $19^{\circ}$ – $20^{\circ}$ C over the western Mediterranean (Fig. 10a), even close to the Catalan coast. Corresponding latent heat flux simulated by the model reaches values as high  $200$ – $300$   $\text{W m}^{-2}$  upstream from Catalonia (Figs. 10b and 6). Therefore, the potential importance of the latent heat flux factor cannot be neglected for this episode and deserves special attention.

Sensitivity experiments were performed with the aim of isolating the effect of the orographic and evaporation factors (sections 4a and 4b, respectively). The sensitivity analysis to the dynamical factors is developed in section 4c. Table 1 summarizes the set of sensitivity experiments.

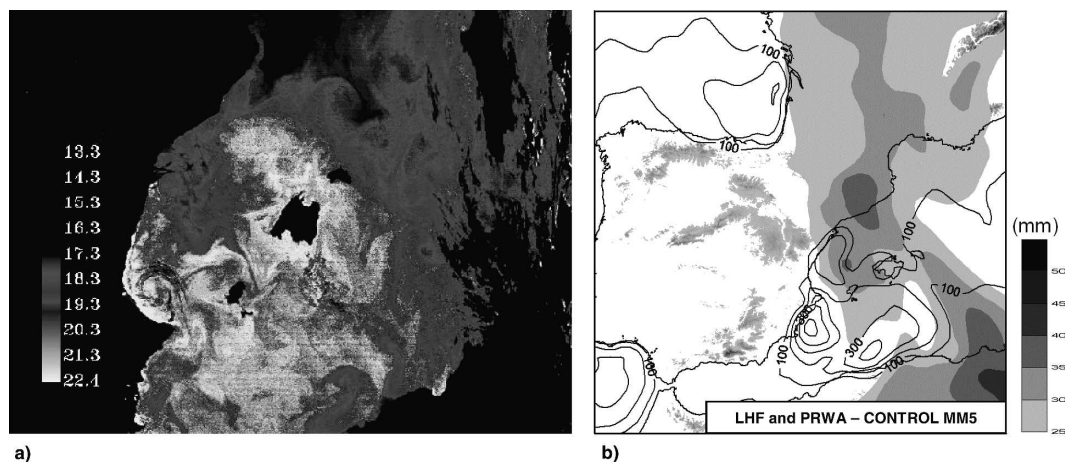


FIG. 10. (a) SST from the *NOAA-14* satellite at 0415 UTC 8 Jun 2000. (b) Control simulation latent heat flux from the sea (continuous line, intervals of  $100$   $\text{W m}^{-2}$ , starting at  $100$   $\text{W m}^{-2}$ ) and precipitable water (shaded according to scale, mm) for the second domain at 0000 UTC 10 Jun 2000. Main orographic systems are highlighted.

TABLE 1. Summary of the numerical experiments performed for the flash flood event in Catalonia according to the methodology described in the text.

Simulations	Type of perturbation
Control	Without perturbation
NO ORO	Flattened orography
NO LHF	Switched-off latent heat flux
PV -25	PV weakened 25%
PV +25	PV intensified 25%
PV 216W	PV moved westward 216 km
PV 216E	PV moved eastward 216 km

*a. Boundary factor (orography)*

To assess the effect of the orography in modifying the mesoscale flow and producing direct lifting, we designed an experiment in which the model orography is flattened to 1 m above sea level. The results of this experiment show that the quasi-stationary mesoscale cyclone identified in the control run (recall Fig. 6), a key player in the flooding event, is weaker and progressing faster to the northeast, thus revealing an apparent connection between the intensity and quasi-stationarity of this feature and the Iberian Peninsula orography. Consequently, the modified orography experiment does not reproduce low-level convergence over Catalonia and the front crosses the region faster than in the control run (Fig. 11). The resulting precipitation amounts are considerably weaker than in the control run (Fig. 12) because of the absence of impinging maritime flow and the lack of orographic ascent that maintained the precipitating systems over the area.

Therefore, the Iberian orography is shown to act primarily by modifying the mesoscale flow and intensifying the cyclone development offshore of eastern Spain through lee cyclogenesis. This enhanced the moist easterly winds inland that converged with the Atlantic front over Catalonia.

*b. Physical factor (latent heat flux)*

The no-evaporation experiment represents a situation in which the latent heat flux from the sea was switched off, thereby removing the continuous water vapor supply to the low levels. In the end, the effect of the evaporation from the sea turned out to be negligible for this simulation. The mesoscale flows, sea level pressure distribution, and accumulated precipitation are not significantly modified when the evaporation from the sea during the simulation time was switched off (results not shown). Therefore, the high moisture content at the initial time (the low-level relative humidity exceeded 60% in the western Mediterranean for the entire simu-

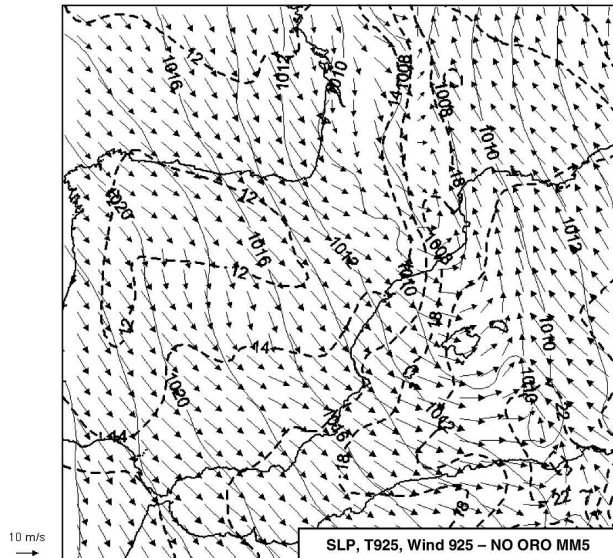


FIG. 11. Same as in Fig. 6 but for the NO ORO experiment.

lation) was sufficient to destabilize the low-level parcels and to ensure continuous moisture supply to the heavy precipitating systems. This explicitly highlights the importance of appropriate humidity fields in order to initialize short-range forecasts of Mediterranean flooding events.

*c. Dynamical factors*

The piecewise potential vorticity (PV) inversion technique was used to analyze the effect of dynamical

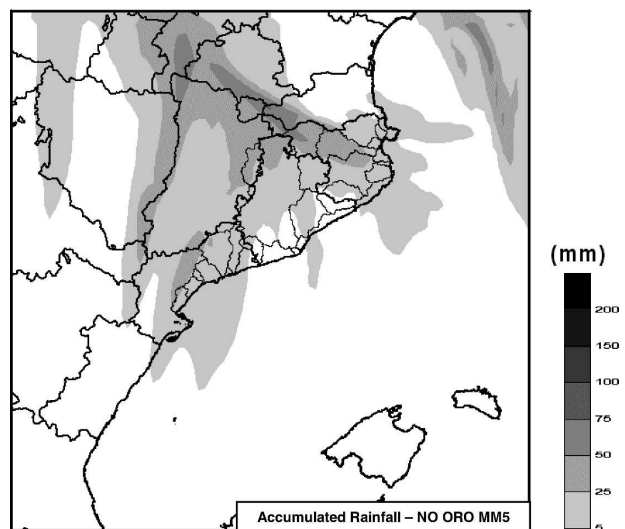


FIG. 12. The NO ORO experiment accumulated rainfall (shaded according to scale, mm) for the third domain at the end of the simulation. Maximum value is 77 mm.

structures identified on the initial conditions fields over the evolution of the event. Provided that the subsynoptic-scale features of the PV field are more prone to analysis errors than the synoptic-scale components, the sensitivity study is focused on the initial intensity and position of the PV center embedded associated with the main cold trough. Moreover, the MM5 adjoint model is used to confirm the notable role of the upper-level disturbance on this event and to reduce the range of possible modifications to the initial PV fields.

### 1) ADJOINT MODEL

An adjoint model can provide valuable guidance by pointing to the PV features that are most likely to be influential for a particular aspect of interest in the forecast. Adjoint models are the transpose of the first-order linear approximation of the evolution of perturbations in the standard forward nonlinear simulations, and so they follow a phase-space trajectory that is tangent linear to the trajectory followed by the basic state. Admittedly, the tangent-linear character limits the validity of its results in the full nonlinear framework, and especially in cases with active convection and heavy precipitating systems. However, adjoint-derived sensitivities become meaningful when the adjoint model is initialized with the appropriate selection of forecast aspects.

We use the MM5 adjoint model (Zou et al. 1997, 1998) developed at NCAR, which has already been applied and tested for a Mediterranean intense cyclone by Homar and Stensrud (2004). The adjoint model includes a limited number of physical parameterization scheme options that, together with the intrinsic tangent-linear approximation, require a careful set up of runs and interpretation of the resulting sensitivities. Moist processes are considered in the adjoint integration. The explicit moisture, including ice concentration, is parameterized using the adjoint of the Dudhia (1989) microphysics scheme, and the Grell et al. (1994) convective scheme is also included. No boundary layer parameterization is available but radiation and surface fluxes are considered. Using this configuration, we provide the model a response function of interest at a certain sensitivity time and it traces back its sensitivity to the initial condition fields.

It is well known that small-scale details of the sensitivity fields computed by the adjoint are very sensitive to the definition of the response function (e.g., Errico 1997). To obtain representative results, it is preferred to define response functions that characterize precursor dynamical systems clearly related to the feature of most interest in the forecast, such as rainfall or convective systems, instead of the feature itself. These forecasted features are likely not well reproduced with the tan-

gent-linear approximation and the adjoint results are less accurate as approximations to the actual sensitivities of the nonlinear standard run. Here, we have defined the response function as the vorticity at the lowest six  $\sigma$  levels (or lowest 100 hPa, approximately) over the center of the mesoscale cyclone that developed offshore northeastern Spain at 0000 UTC 10 June 2000. The adjoint model is initialized with this response function and its sensitivity to the initial condition fields is computed.

The adjoint produces a sensitivity field for each of the model fields: temperature, horizontal wind components, pressure perturbation, and specific humidity. To summarize the three-dimensional sensitivity fields and to provide direct guidance to the piecewise PV inversion technique described in next section, the sensitivity to the quasigeostrophic PV (QPV) is derived from the adjoint variables. In the quasigeostrophic framework, PV is expressed as a function of the geostrophic streamfunction as

$$q = \nabla_p^2 \psi + f_0 + f_0^2 \partial_p \left( \frac{1}{\sigma_r} \partial_p \psi \right), \quad (1)$$

where  $q$  is the QPV,  $\psi$  is the geostrophic streamfunction,  $\sigma_r(p)$  is the stability parameter for a reference state that depends only on  $p$ , and  $f_0$  is the Coriolis parameter. Transposing the discretized version of this equation, and using the relationship between the adjoint variables  $\hat{u}$ ,  $\hat{v}$ , and  $\hat{\psi}$  ( $\hat{\psi} = \partial_y \hat{u} - \partial_x \hat{v}$ ), an elliptic equation for  $\hat{q}$  is obtained:

$$\nabla_p^2 \hat{q}_k + \gamma_1 \hat{q}_k + \gamma_2 \hat{q}_{k+1} - \gamma_3 \hat{q}_{k-1} = \partial_y \hat{u} - \partial_x \hat{v}, \quad (2)$$

where the  $\gamma_x$  parameters depend on the discretization scheme for (1) and are proportional to the inverse of the reference stability parameter  $\sigma_r$  and to its vertical derivative ( $\partial_p \sigma_r$ ). Solving (2) iteratively, the sensitivities of the response functions to modifications in the QPV fields are derived from the adjoint model variables  $\hat{u}$ ,  $\hat{v}$ .

The sensitivity calculations are run on the mother domain of the control experiment for this episode. The sensitivity field to the QPV at the 330-K isentropic surface (Fig. 13) exhibits an elongated distribution of PV and the associated sensitivity patterns point primarily to the west and south sides. Areas with positive (negative) values of sensitivity would increase (decrease) the vorticity of the forecasted mesoscale cyclone when the initial conditions of the simulation were perturbed with positive PV anomalies. The obtained distribution of sensitivities is reasonable and consistent with the previously described evolution of the synoptic pattern, as these areas with high sensitivity evolve with the trough and are later likely involved in the definition of the

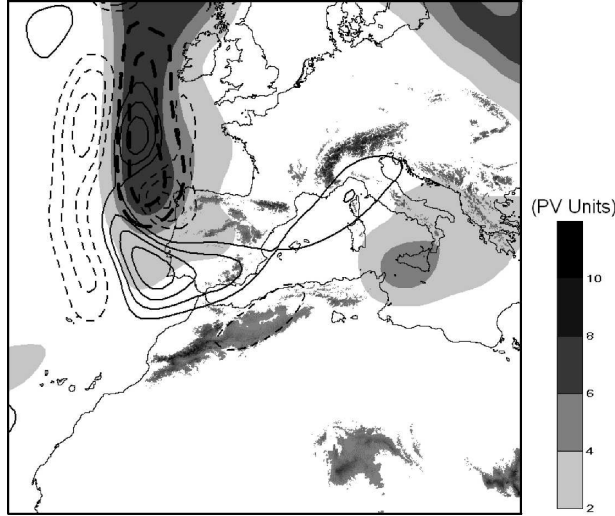


FIG. 13. Isentropic PV on the 330-K surface (shaded according to scale, PV units) and main areas of sensitivity at the same isentropic surface (continuous line, positive values; dashed line, negative values) for the selected response function (see text) at 0000 UTC 9 Jun 2000. The thick dashed line represents the PV anomaly (contours correspond to four and six PV units) that was inverted to construct the perturbed simulations shown on the 330-K surface. Main orographic systems are highlighted.

particular low-level flow associated with the Mediterranean cyclogenesis. Figure 13 also shows areas with notable sensitivity far to the east of the trough, over the western Mediterranean. Because these sensitivity structures are not related to the intense trough-related PV streamer in the initial analysis, their physical interpretation is not clear. This might be an indirect effect on the eastward progression of the main trough, but we have no direct evidence to support this speculation.

In summary, the adjoint results highlight various aspects of the precursor upper-level trough, with special emphasis on its location and intensity. Provided that the precise details of the sensitivity field are unreliable because of the approximations used, the sensitivity analysis suggests that the precursor upper-level trough is important and motivates additional sensitivity experiments focused on its location and intensity (Table 1).

## 2) PIECEWISE POTENTIAL VORTICITY INVERSION METHOD

The method used to explore the sensitivity of the mesoscale simulation to the upper-level trough PV center associated with the trough, requires the calculation of a balanced flow associated with the anomaly that can be used to alter the model initial conditions in a physically consistent way without introducing any significant noise. The piecewise PV inversion technique of Davis

and Emanuel (1991) has been used for such purpose. The method starts with the calculation of the balanced flow, described  $\phi$  (geopotential) and  $\psi$  (streamfunction), from the total or instantaneous distribution of Ertel's potential vorticity  $q$  (see Rossby 1940; Ertel 1942), given by the following expression:

$$q = \frac{1}{\rho} \boldsymbol{\eta} \cdot \nabla \theta, \quad (3)$$

where  $\rho$  is the density,  $\boldsymbol{\eta}$  is the absolute vorticity vector, and  $\theta$  is the potential temperature. The balance assumption made follows the Charney (1955) nonlinear balance equation:

$$\nabla^2 \phi = \nabla \cdot f \nabla \psi + 2m^2 \left[ \frac{\partial^2 \psi}{\partial x^2} \frac{\partial^2 \psi}{\partial y^2} - \left( \frac{\partial^2 \psi}{\partial x \partial y} \right)^2 \right], \quad (4)$$

where  $f$  is the Coriolis parameter and  $m$  denotes the map scale factor of the particular  $(x, y)$  projection used. The other diagnostic relation necessary for the inversion of  $\phi$  and  $\psi$  is given by the approximate form of (3), resulting from the hydrostatic assumption and the same scale analysis used to derive (4); namely, that the irrotational component of the wind is very small relative to the nondivergent wind:

$$q = \frac{g\kappa\pi}{p} \left[ (f + m^2 \nabla^2 \psi) \frac{\partial^2 \phi}{\partial^2 \pi} - m^2 \left( \frac{\partial^2 \psi}{\partial x \partial \pi} \frac{\partial^2 \phi}{\partial x \partial \pi} + \frac{\partial^2 \psi}{\partial y \partial \pi} \frac{\partial^2 \phi}{\partial y \partial \pi} \right) \right], \quad (5)$$

where  $p$  is the pressure,  $g$  is the gravity,  $k = R_d/C_p$ , and the vertical coordinate  $\pi$  is the Exner function  $C_p(p/p_0)^k$ . The finite-difference form of the closed system described by (4) and (5) is solved for the unknowns  $\phi$  and  $\psi$  given  $q$ , using an iterative technique until convergence of the solutions is reached (refer to Davis and Emanuel 1991, for the details). Neumann-type conditions ( $\partial\phi/\partial\pi = f\partial\psi/\partial\pi = -\theta$ ) are applied on the top and bottom boundaries, and Dirichlet conditions on the lateral boundaries. The latter are supplied by the observed geopotential and a streamfunction calculated by matching its gradient along the edge of each isobaric surface to the observed normal wind component, which is first slightly modified to force no net divergence in the domain. Because of the balance condition used, the inverted fields are very accurate even for meteorological systems characterized by large Rossby numbers (see Davis and Emanuel 1991; Davis 1992).

Next, a reference state must be found from which to define perturbations. As in Davis and Emanuel (1991), this reference state is defined as a time average. Given  $\bar{q}$ , the time mean of  $q$ , a balanced mean flow  $(\bar{\phi}, \bar{\psi})$  is

inverted from identical equations to (4) and (5), except all dependent variables are mean values and the mean potential temperature  $\bar{\theta}$  is used for the top and bottom boundary conditions. The perturbations fields ( $q'$ ,  $\phi'$ ,  $\psi'$ ) are given by the following definition:

$$(q, \phi, \psi) = (\bar{q}, \bar{\phi}, \bar{\psi}) + (q', \phi', \psi'). \quad (6)$$

Finally, we can consider that the PV perturbation field  $q'$  is partitioned into  $N$  portions or anomalies  $q' = \sum_{n=1}^N q_n$ . We are interested in obtaining that part of the flow ( $\phi_n, \psi_n$ ) associated with each PV portion  $q_n$ , and

we also require  $\phi' = \sum_{n=1}^N \phi_n$  and  $\psi' = \sum_{n=1}^N \psi_n$ . As discussed in Davis (1992), there is no unique way to define a relationship between  $(\phi_n, \psi_n)$  and  $q_n$  because of the nonlinearities present in (4) and (5). Here, we adopt the linear method of Davis and Emanuel (1991), derived after substitution of expression (6) and the above summations in (4) and (5) and equal partitioning of the nonlinear term among the other two linear terms that result from each nonlinearity in the above equations. The resulting linear closed system for the  $n$ th perturbation is

$$\nabla^2 \phi_n = \nabla \cdot f \nabla \psi_n + 2m^2 \left( \frac{\partial^2 \psi^*}{\partial x^2} \frac{\partial^2 \psi_n}{\partial y^2} + \frac{\partial^2 \psi^*}{\partial y^2} \frac{\partial^2 \psi_n}{\partial x^2} - 2 \frac{\partial^2 \psi^*}{\partial x \partial y} \frac{\partial^2 \psi_n}{\partial y \partial x} \right), \quad (7)$$

$$q_n = \frac{g\kappa\pi}{p} \left[ \begin{array}{l} (f + m^2 \nabla^2 \psi^*) \frac{\partial^2 \phi_n}{\partial \pi^2} + m^2 \frac{\partial^2 \phi^*}{\partial \pi^2} \nabla^2 \psi_n \\ - m^2 \left( \frac{\partial^2 \phi^*}{\partial x \partial \pi} \frac{\partial^2 \psi_n}{\partial x \partial \pi} + \frac{\partial^2 \phi^*}{\partial y \partial \pi} \frac{\partial^2 \psi_n}{\partial y \partial \pi} \right) - m^2 \left( \frac{\partial^2 \psi^*}{\partial x \partial \pi} \frac{\partial^2 \phi_n}{\partial x \partial \pi} + \frac{\partial^2 \psi^*}{\partial y \partial \pi} \frac{\partial^2 \phi_n}{\partial y \partial \pi} \right) \end{array} \right], \quad (8)$$

where  $(\ )^* = \bar{(\ )} + 1/2(\ )$ . The system (7)–(8) is solved for the nucleus of the upper-level (above 500 hPa) positive PV anomaly associated with the precursor trough, defined at 0000 UTC 9 June 2000 as the departure from a 7-day mean centered at the same time. Figure 13 shows its structure on the 330-K surface. The corresponding balance fields were subtracted and/or added to MM5 initial fields to construct the new sensitivity experiments indicated in Table 1.

### 3) SENSITIVITY TO INTENSIFYING/WEAKENING THE DISTURBANCE'S AMPLITUDE AT UPPER LEVELS

The adjoint computes the most sensitive areas at upper levels of the mesoscale cyclone east of mainland Spain 24 h in the forecast, around the PV ridge. In particular, the sensitivity fields focus on the westward and southern gradient as well as on the intensity of the PV anomaly (Fig. 13). The adjoint sensitivities must be interpreted carefully and confirmed with the corresponding standard MM5 experiments. Therefore, we have tested the sensitivity of the forecast fields to changes in the position and intensity of the upper-level positive PV anomaly.

In a first experiment, the PV anomaly is weakened by 25%. The modified initial condition fields produce a shallower cold upper-level trough (Fig. 14a). As a result, the pattern at upper levels evolves more slowly than the control run. Because this episode was linked to rapid cyclogenesis in response to the upper-level forcing, the low-level cyclone still develops, although

weaker and centered more to the southwest (Fig. 15a). The mesoscale cyclone in this experiment is less intense but more stationary than in the control run. Therefore, as a consequence of its enhanced stagnancy and the southwest displacement of the moisture convergence owing to the modified mesoscale cyclone's location, the low-level warm moist inflow from the Mediterranean Sea persists longer, increasing the total accumulated rainfall to a maximum value of 214 mm and shifting the main rainfall band about 150–200 km south of the actual affected zones (Fig. 16a).

On the other hand, the experiment with the PV anomaly intensified by 25% shows a deeper and colder upper-level trough (Fig. 14b) that moves eastward faster than the control one. The resultant low-level mesoscale cyclone is slightly more intense and its displacement along the Spanish eastern coast into southern France is also more rapid (Fig. 15b). However, although the synoptic-scale forcings are stronger than in the control simulation, the accumulated precipitation is lower (maximum value is 115 mm, Fig. 16b). In addition, the spatial distribution of the precipitation field is clearly different and shifted to the north. These differences are related to the faster movement of the mesoscale cyclone that does not allow for a stationary and continuous supply of warm moist air toward Catalonia.

Therefore, the intensity of the precursor PV system appears crucial as to predict flooding potential in the densely populated Barcelona province. Neither stronger nor weaker PV anomalies produce higher amounts

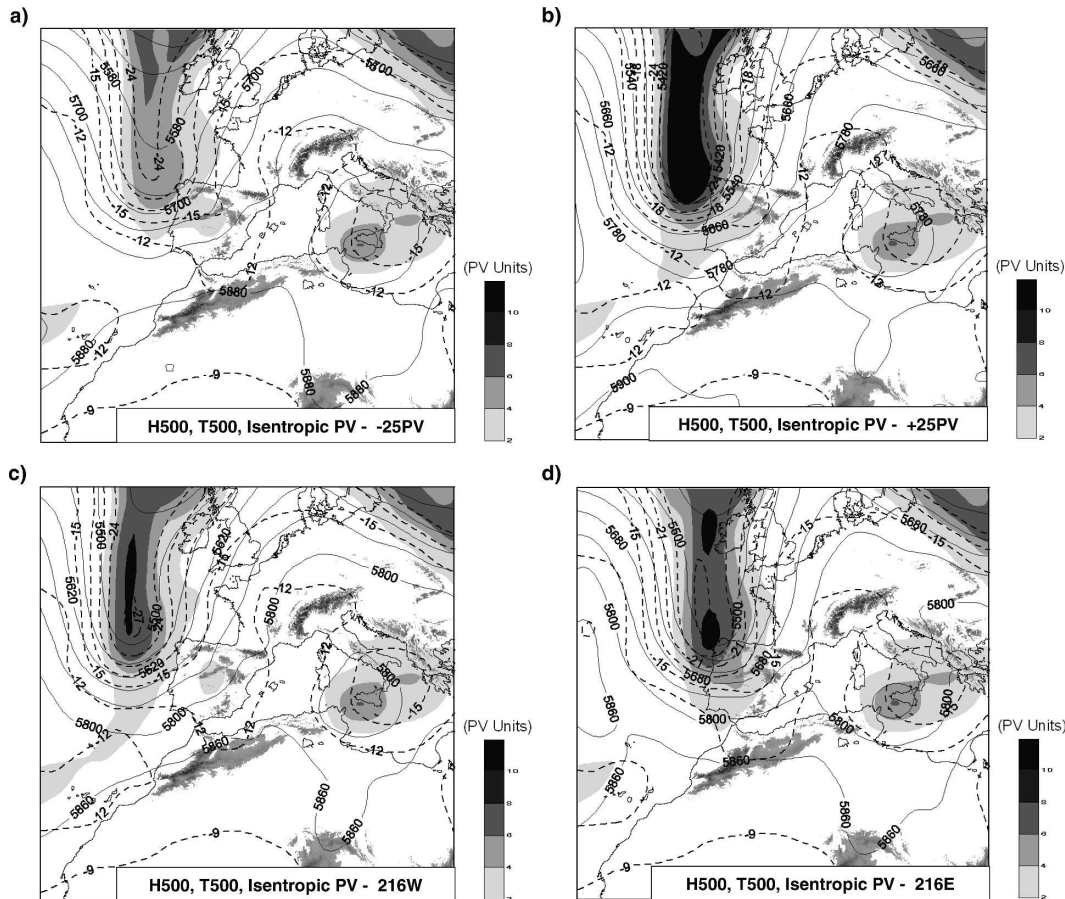


FIG. 14. Perturbed simulations: Geopotential height at 500 hPa (continuous line, gpm), temperature at 500 hPa (dashed line, °C) and isentropic PV on the 330-K surface (shaded according to scale, PV units) for the coarse domain at 0000 UTC 9 Jun 2000 and for the experiments: (a) PV -25, (b) PV +25, (c) PV 216W, and (d) PV 216E. Main orographic systems are highlighted.

of accumulated rainfall than the control run in that area, owing to the peculiar mesoscale coincidences that lead to the actual torrential rains.

#### 4) SENSITIVITY TO DISPLACING THE DISTURBANCE AT UPPER LEVELS

The sensitivity of the forecast to the gradients of the precursor upper-level PV anomaly was considered by designing two experiments where the position of the anomaly was shifted along the “west–east” model coordinate. A displacement of 216 km (four grid points) reflects a representative error over an area with few in situ observations and where analyses rely mainly on previous model forecasts (Figs. 14c,d). Surprisingly enough, the response of the simulated low-level mesoscale cyclone is quasi-linearly related to the shifts in location of the precursor PV anomaly. When the PV anomaly was shifted west (east), the mesoscale cyclone and the associated circulation were also shifted west

(east), keeping almost the same translational speed as in the control run (Figs. 15c,d).

Regarding the precipitation fields, when the mesoscale cyclone was shifted inland, the circulation interacted with the local topography (Fig. 15c) and the precipitation pattern was similar to the control run (maximum value is 177 mm), but with the highest amounts shifted inland (Fig. 16c). When the system was shifted eastward, the cyclone developed too far from the Catalan coast (Fig. 15d) and the impinging warm and moist Mediterranean air was not persistent. As a consequence, the amount of the forecast rainfall was substantially reduced (maximum value is 113 mm) and a large part of it fell over the Mediterranean Sea (Fig. 16d).

### 5. Conclusions

A case of severe flooding occurred in June 2000 over Catalonia killing 5 people and affecting 500 people. The

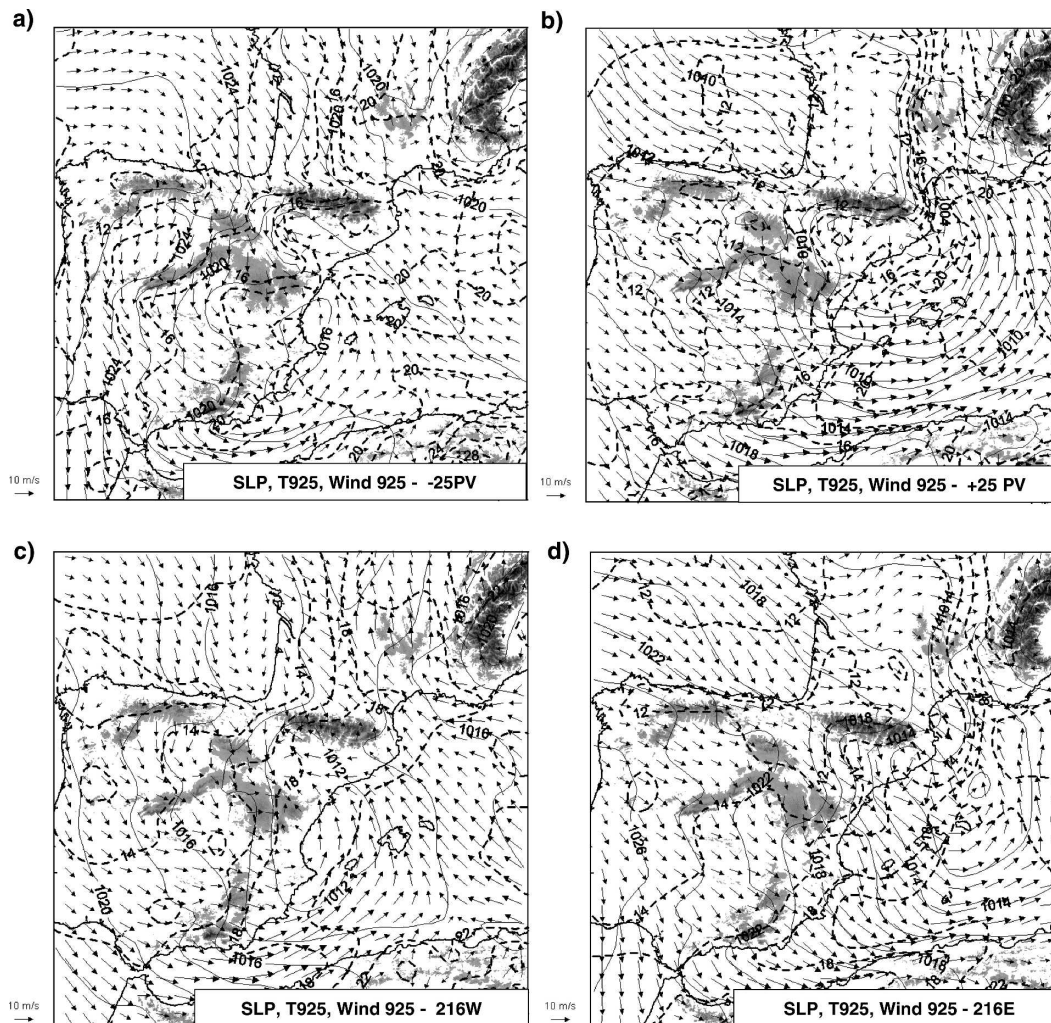


FIG. 15. Perturbed simulations: Same as in Fig. 6 for the experiments: (a) PV  $-25$ , (b) PV  $+25$ , (c) PV  $216W$ , and (d) PV  $216E$ .

36-h rainfall generally exceeded 40 mm across the region, and more than 200 mm was registered close to the Montserrat monastery. The analysis of the available observations shows active convection during the night of 9–10 June 2000 moving along an Atlantic front that crossed the Iberian Peninsula. Persistent warm and moist southeasterly flow was produced during the night because of secondary cyclogenesis, reinforced by orographically forced flows leeward of the Pyrenees. Radar images show the frontal convective activity and the merging of two MCSs that remained quasi-stationary, producing the highest rainfall intensities for this event.

Numerical sensitivity experiments have revealed various important aspects regarding the predictability of this kind of western Mediterranean flash flood events. The intensity, location, and the circulation associated with the mesoscale cyclone located east of

mainland Spain is shown to be driven by the regional orography, which anchors the system leeward of the Iberian Peninsula and generates the southeasterly moist flow that later converges with the Atlantic front. The accuracy of the initial condition fields has been shown to be very important with three kinds of experiments. First, low-level humidity in the initial conditions regulates the predicted rainfall amounts, but with negligible contribution in this case from the sea surface fluxes. Second, the location of the upper-level precursor PV anomaly modulates the position of the low-level mesoscale cyclone 24 h in the forecast, which also shifts the location of the heavy rainfall. Third, the intensity of the precursor trough is shown to modify this feature's translational speed, preventing the mesoscale cyclone from remaining quasi-stationary offshore and inducing the persistent maritime flow toward Catalonia.

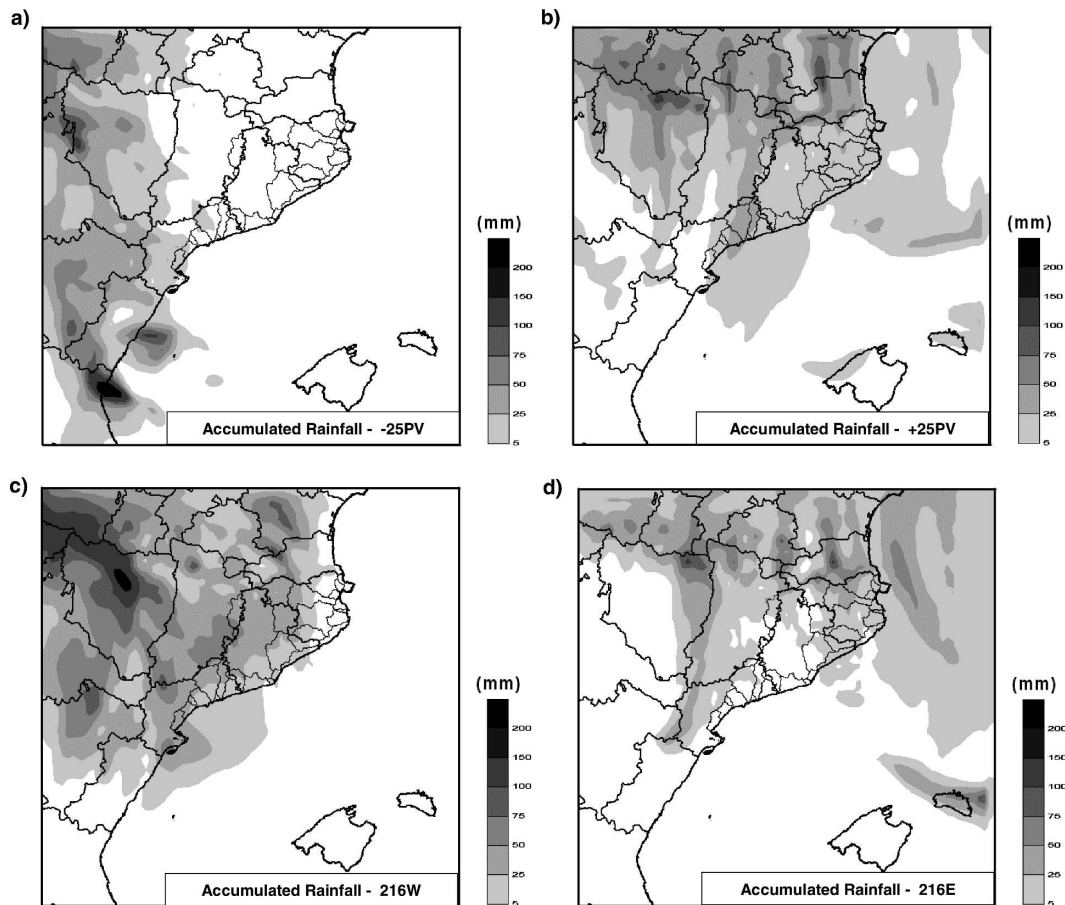


FIG. 16. Perturbed simulations: Same as in Fig. 9a for the experiments: (a) PV  $-25$  (max value is 214 mm), (b) PV  $+25$  (max value is 115 mm), (c) PV 216W (max value is 177 mm), and (d) PV 216E (max value is 113 mm).

Therefore, all tested modifications of the precursor upper-level system altered the conditions conducive to heavy precipitation, highlighting the peculiar set of circumstances that had to occur for the high impact episode to develop. The high sensitivity of the location and intensity of the 36-h predicted rainfall to changes in the upper-level dynamical precursor reveals the limited predictability of this kind of episode. Indeed, it is remarkable that by taking the four experiments with modified PV anomalies as a grossly generated four-member ensemble prediction system, only one member would be considered as predicting heavy rainfall forecasts in the area. This illustrates the problem of dealing with high mesoscale variability resulting from a set of perturbed simulations in the synoptic scale, and the difficulty in producing a valuable probabilistic mesoscale forecast out of the ensemble system.

Although the control run with the MM5 model in research mode predicted the location and intensity of the damaging rains with high accuracy for this episode, the operational forecast of similar events should be

viewed with extreme caution, because a number of conditions, some of them with very limited predictability, have to occur in order to produce heavy rains and the consequent flash floods.

*Acknowledgments.* This research was developed under the objectives and financial support of Spanish Project MEDEXIB (REN2002-03482/CLI) and Interreg IIIB-Medoc European project HYDROPTIMET (2002-02-4.3-I-079). Radar images and rain gauge network data of Aragon, Catalonia, the Balearic Islands, and Valencia were provided by the Instituto Nacional de Meteorología (INM) of Spain. The AVHRR image was supplied in the HRPT-1b format by the Satellite Receiving Station from Dundee University. Automatic rain gauge network data of the Internal Basins of Catalonia were given by the Agencia Catalana del Agua (ACA) of Catalonia. The NCAR Scientific Computer Division (sponsored by the National Science Foundation) is acknowledged for providing access to NCEP analyses. Our colleagues from the Meteorology Group

of the Balearic Islands University, L. F. Borrell and A. M. Navarro are acknowledged for their help in producing Figs. 8 and 10a, respectively. We are very grateful to the three reviewers, especially C. Doswell, for their comments and corrections that helped to notably improve the manuscript.

## REFERENCES

- Anthes, R. A., and T. T. Warner, 1978: Development of hydrodynamic models suitable for air pollution and other meso-meteorological studies. *Mon. Wea. Rev.*, **106**, 1045–1078.
- Benjamin, S. B., and N. L. Seaman, 1985: A simple scheme for improved objective analysis in curved flow. *Mon. Wea. Rev.*, **113**, 1184–1198.
- Buzzi, A., N. Tartaglione, and P. Malguzzi, 1998: Numerical simulations of the 1994 Piedmont flood. Role of orography and moist processes. *Mon. Wea. Rev.*, **126**, 2369–2383.
- Charney, J. G., 1955: The use of primitive equations of motion in numerical prediction. *Tellus*, **7**, 22–26.
- Davis, C. A., 1992: Piecewise potential vorticity inversion. *J. Atmos. Sci.*, **49**, 1397–1411.
- , and K. A. Emanuel, 1991: Potential vorticity diagnosis of cyclogenesis. *Mon. Wea. Rev.*, **119**, 1929–1953.
- Delitala, A. M. S., M. Casula, and G. Ficca, 2002: Intense precipitation over Sardinia during MEDEX case of 25–31 December 2002. *Proc. Fourth EGS Plinius Conf. on Mediterranean Storms*, Mallorca, Spain, Universitat de les Illes Balears, CD-ROM, Session 1.
- Doswell, C. A., C. Ramis, R. Romero, and S. Alonso, 1998: A diagnostic study of three heavy precipitation episodes in the western Mediterranean region. *Wea. Forecasting*, **13**, 102–104.
- Dudhia, J., 1989: Numerical study of convection observed during the winter monsoon experiment using a mesoscale two-dimensional model. *J. Atmos. Sci.*, **46**, 3077–3107.
- Errico, R. M., 1997: What is an adjoint model? *Bull. Amer. Meteor. Soc.*, **78**, 2577–2591.
- Ertel, H., 1942: Ein neuer hydrodynamischer wirbelsatz. *Meteor. Z.*, **59**, 271–281.
- Fernández, C., M. A. Gaertner, C. Gallardo, and M. Castro, 1995: Simulation of a long-lived meso- $\beta$  scale convective system over the Mediterranean coast of Spain. Part I: Numerical predictability. *Meteor. Atmos. Phys.*, **56**, 157–179.
- Font, I., 1983: *Climatology of Spain and Portugal* (in Spanish). Instituto Nacional de Meteorología, 296 pp.
- Grell, G. A., J. Dudhia, and D. R. Stauffer, 1994: A description of the fifth-generation Penn State/NCAR Mesoscale Model (MM5). NCAR Tech. Note NCAR/TN-398+STR, 125 pp.
- Homar, V., and D. J. Stensrud, 2004: Sensitivities of an intense cyclone over the western Mediterranean. *Quart. J. Roy. Meteor. Soc.*, **130**, 2519–2540.
- , C. Ramis, R. Romero, S. Alonso, J. A. García-Moya, and M. Alarcón, 1999: A case of convection development over the western Mediterranean Sea: A study through numerical simulations. *Meteor. Atmos. Phys.*, **71**, 169–188.
- , R. Romero, C. Ramis, and S. Alonso, 2002: Numerical study of the October 2000 torrential precipitation event over eastern Spain: Analysis of the synoptic-scale stationarity. *Ann. Geophys.*, **20**, 2047–2066.
- , M. Gayà, R. Romero, C. Ramis, and S. Alonso, 2003a: Tornadoes over complex terrain: An analysis of the 28th August 1999 tornadic event in eastern Spain. *Atmos. Res.*, **67–68**, 301–317.
- , R. Romero, D. J. Stensrud, C. Ramis, and S. Alonso, 2003b: Numerical diagnosis of a small, quasi-tropical cyclone over the western Mediterranean: Dynamical vs. boundary factors. *Quart. J. Roy. Meteor. Soc.*, **129**, 1469–1490.
- Hong, S.-Y., and H.-L. Pan, 1996: Non-local boundary layer vertical diffusion in a medium-range forecast model. *Mon. Wea. Rev.*, **124**, 2322–2339.
- Kain, J. S., and J. M. Fritsch, 1993: Convective parameterization for mesoscale models: The Kain–Fritsch scheme. *The Representation of Cumulus Convection in Numerical Models*, Meteor. Monogr., No. 46, Amer. Meteor. Soc., 165–170.
- Langland, R. H., R. Gelaro, G. D. Rohaly, and M. Shapiro, 1999a: Targeted observations in fastex: Adjoint-based targeting procedures and data impact experiments in IOP17 and IOP18. *Quart. J. Roy. Meteor. Soc.*, **125**, 3241–3270.
- Llasat, M. C., 2001: An objective classification of rainfall events on the basis of their convective features. Application to rainfall intensity in the North-East of Spain. *Int. J. Climatol.*, **21**, 1385–1400.
- , F. Martín, O. Carretero, T. Rigo, and J. De Batlle, 2002: Diagnosis of a strong convective event produced in Catalonia on June 10, 2000. *Proc. Third EGS Plinius Conf.*, Publ. 2560, Baja Sardinia, Italy, GNDCI, 67–70.
- , M. Barriendos, and T. Rigo, 2003: The “Montserrat-2000” flash-flood event: A comparison with the floods that have occurred in the Northeast Iberian Peninsula since the 14th century. *Int. J. Climatol.*, **23**, 453–469.
- Mlawer, E. J., S. J. Taubman, P. D. Brown, M. J. Iacono, and S. A. Clough, 1997: Radiative transfer for inhomogeneous atmospheres: RRTM, a validated correlated-k model for the longwave. *J. Geophys. Res.*, **102**, 16 663–16 682.
- Ramis, C., R. Romero, V. Homar, S. Alonso, and M. Alarcón, 1998: Diagnosis and numerical simulation of a torrential precipitation event in Catalonia (Spain). *Meteor. Atmos. Phys.*, **69**, 1–21.
- , —, —, and —, 2001: Heavy rainfalls (in Spanish). *Investig. Cienc.*, **296**, 60–68.
- Reisner, J., R. J. Rasmussen, and R. T. Bruintjes, 1998: Explicit forecasting of supercooled liquid water in winter storms using the MM5 mesoscale model. *Quart. J. Roy. Meteor. Soc.*, **124B**, 1071–1107.
- Riesco, J., J. Tamayo, and V. Alcover, 2002: Heavy maritime rainfall in the Valencia Region: The 6 to 8 May 2002 situation. *Proc. Fourth EGS Plinius Conf. on Mediterranean Storms*, Mallorca, Spain, Universitat de les Illes Balears, CD-ROM, Session 1.
- Romero, R., 2001: Sensitivity of a heavy rain producing Western Mediterranean cyclone to embedded potential vorticity anomalies. *Quart. J. Roy. Meteor. Soc.*, **127**, 2559–2597.
- , C. Ramis, and S. Alonso, 1997: Numerical simulations of an extreme rainfall event in Catalonia: Role of orography and evaporation from the sea. *Quart. J. Roy. Meteor. Soc.*, **123**, 537–559.
- , —, and J. A. Guijarro, 1999: Daily rainfall patterns in the Spanish Mediterranean area: An objective classification. *Int. J. Climatol.*, **19**, 95–112.
- , C. A. Doswell, and C. Ramis, 2000: Mesoscale numerical study of two cases of long-lived quasistationary convective systems over eastern Spain. *Mon. Wea. Rev.*, **128**, 3731–3751.
- Rossby, C. G., 1940: Planetary flow patterns in the atmosphere. *Quart. J. Roy. Meteor. Soc.*, **66** (Suppl.), 68–87.

- Troen, I., and L. Mahrt, 1986: A simple model of the atmospheric boundary layer: Sensitivity to surface evaporation. *Bound.-Layer Meteor.*, **37**, 129–148.
- Weiss, S. J., J. S. Kain, J. J. Levit, M. E. Baldwin, and D. R. Bright, 2004: Examination of several different versions of the Weather Research and Forecasting (WRF) model for the prediction of severe convective weather: The SPC/NSSL Spring Program 2004. Preprints, *22d Conf. on Severe Local Storms*, Hyannis, MA, Amer. Meteor. Soc., CD-ROM, 17.1.
- Xu, M., D. J. Stensrud, J. W. Bao, and T. T. Warner, 2001: Applications of the adjoint technique to short-range ensemble forecasting of mesoscale convective systems. *Mon. Wea. Rev.*, **129**, 1395–1418.
- Zou, X., F. Vandenberghe, M. Ponca, and Y.-H. Kuo, 1997: Introduction to adjoint techniques and the MM5 adjoint modeling system. NCAR Tech. Note NCAR/TN-435+IA, 120 pp.
- , W. Huang, and Q. Xiao, 1998: A user's guide to the MM5 adjoint modeling system. NCAR Tech. Note NCAR/TN-437+IA, 45 pp.

Copyright of *Monthly Weather Review* is the property of American Meteorological Society and its content may not be copied or emailed to multiple sites or posted to a listserv without the copyright holder's express written permission. However, users may print, download, or email articles for individual use.